

DR. XUANWEN BAO (Orcid ID : 0000-0002-6232-3783)

DR. MICHAEL ROSEMANN (Orcid ID : 0000-0002-5855-065X)

Received Date : 15-Jan-2020

Revised Date : 15-Apr-2020

Accepted Date : 22-Apr-2020

Article type : Research Article

Extended *in vitro* culture of primary human mesenchymal stem cells downregulates *Brca1*-related genes and impairs DNA double-strand break recognition

Xuanwen Bao ^{1,2}, Jing Wang ^{1,2}, Guangming Zhou ³, Attila Aszodi ⁴, Veronika Schönitzer ⁴, Harry Scherthan ⁵, Michael J. Atkinson ^{1,6}, Michael Rosemann ^{1,2,*}

This article has been accepted for publication and undergone full peer review but has not been through the copyediting, typesetting, pagination and proofreading process, which may lead to differences between this version and the [Version of Record](#). Please cite this article as [doi: 10.1002/2211-5463.12867](https://doi.org/10.1002/2211-5463.12867)

FEBS Open Bio (2020) © 2020 The Authors. Published by FEBS Press and John Wiley & Sons Ltd.

This is an open access article under the terms of the Creative Commons Attribution License, which permits use, distribution and reproduction in any medium, provided the original work is properly cited.

(1) Institute of Radiation Biology, Helmholtz Center Munich - German Research Center for Environmental Health, Ingolstaedter Landstr. 1, 85764 Neuherberg, Germany

(2) Medical Graduate School, Technical University of Munich, 81675 Munich, Germany

(3) State Key Laboratory of Radiation Medicine and Protection, School of Radiation Medicine and Protection, Medical College of Soochow University, Suzhou, China

(4) Laboratory of Experimental Surgery and Regenerative Medicine, Clinic for General, Trauma and Reconstructive Surgery, Ludwig-Maximilians University, 80336 Munich, Germany

(5) Bundeswehr Institute of Radiobiology, affil. to the Univ. of Ulm, Neuherbergstr. 11, 80937 Munich, Germany

(6) Chair of Radiation Biology, Technical University of Munich, 81675 Munich, Germany

(*) Corresponding author: Dr. Michael Rosemann, Institute of Radiation Biology, Helmholtz Center Munich - German Research Center for Environmental Health, Ingolstaedter Landstr. 1, 85764 Neuherberg, Germany
Tel +49-(0)89-31872628, e-mail: rosemann@helmholtz-muenchen.de

Keywords: Mesenchymal stem cells (MSCs); cellular aging; DNA repair; homologous recombination; *BRCA1*

Abbreviations

MSC: Mesenchymal stem cell/Mesenchymal stroma cell

DDR: DNA damage response

hBM-MSC: human Bone marrow derived mesenchymal stem cell

BAM: binary sequence alignment map file

GO: gene ontology

GSEA: Gene set enrichment analysis

DSB: double strand break

qRT-PCR: quantitative real-time polymerase chain reaction

HR: homologous recombination

IPA: Ingenuity pathway analysis

CNV: DNA copy number variation

Running heading:

DNA repair by HR in ex-vivo aging human MSCs

Abstract: Mesenchymal stem cells (MSCs) are multi-lineage adult stem cells with considerable potential for cell based regenerative therapies. *In vitro* expansion changes their epigenetic and cellular properties, with a poorly understood impact on DNA damage response and genome stability. We report here results of a transcriptome-based pathway analysis of *in vitro* expanded hBM-MSCs, supplemented with cellular assays focusing on DNA double-strand break (DSB) repair. Gene pathways affected by *in vitro* aging were mapped using gene ontology, KEGG, GSEA, and were found to involve DNA repair, homologous recombination, cell cycle control and chromosomal replication. Assays for the recognition (γ -H2AX+53BP1 foci) and repair (pBRCA1+ γ -H2AX foci) of X-ray induced DNA DSBs in hBM-MSCs show that over a period of 8 weeks of *in vitro* aging (i.e. about 10 doubling times), cells exhibit a reduced DNA damage response and a higher fraction of residual DNA damage. Furthermore, a distinct sub-population of cells with impaired DNA DSB recognition was observed. Several genes which participate in DNA repair by homologous recombination (e.g., Rad51, Rad54, BRCA1) show a 2.3 to 4 fold reduction of their mRNA expression by qRT-PCR. We conclude that the *in vitro* expansion of hMSCs can lead to aging-related impairment of the recognition and repair of DNA breaks.

Introduction

Mesenchymal stem or mesenchymal stromal cells (MSCs) are adult stem cells that reside in bone marrow stroma and other connective tissues. Their lifelong potential to generate committed precursor cells for various lineages is essential for both the continued replacement of cellular losses and for the recovery of connective tissue damage. In addition to their role as a stem cell pool MSCs are also a source for immunomodulatory paracrine factors, thereby serving as a regulator of inflammation and immune response [1, 2]. The possibility to expand donor- and patient-derived MSCs *in vitro* and to induce a selected differentiation program prior to an autologous or allogenic implantation makes them highly attractive for cell-based therapies [3, 4].

The procedure for *in vitro* expansion of MSCs is not yet optimized. Cellular stressors, such as excessive oxygen levels or exposure to low-dose irradiation can impair the natural function of MSCs during the subsequent *in vitro* expansions required for transplantation [5, 6]. Sources of

genotoxic stress can be as various as repeated diagnostic radiology, therapeutic radiation applications or long-lasting low-level exposures to environmental or occupational noxae, both in the form of ionizing radiation or of chemicals that form DNA damaging radical. One common problem during *in vitro* expansion of MSCs is the appearance of cellular senescence, characterized by a gradual loss of their proliferative capacity and their multipotency [7, 8]. The age and health status of MSC donors also have an influence on the long-term proliferative capacity of *in vitro* expanded MSCs. The loss of stemness and increased senescence are associated with changes in epigenetic DNA marks [8-10]. Investigating the detrimental influence of oxidative stress on proliferation and DNA damage response of bone-marrow derived human MSC Bigot et al observed that a reduced oxygen environment results in a higher initial clonogenicity, a less-pronounced loss of colony numbers with increasing passage numbers and a higher baseline expression of the DNA repair protein RAD51. [11]. They could also show that under reduced O₂ chemically induced DNA double-strand breaks are repaired more efficient, with γ -H2AX foci going back to nearly control level after 24h repair incubation. Considering that oxidative stress is indeed a major factor causing cellular aging one could speculate that their data indeed suggest an age-related change in DNA repair.

The long residency of MSCs in tissues, and the fact that they cannot be regenerated from more primitive cells, makes MSCs vulnerable to the accumulation of DNA damage by chronic genotoxic stress. Some studies suggest that hMSCs are relatively radio resistant, even after higher radiation doses [12, 13]. MSCs are not prone to radiation-induced apoptosis, and their robust clonogenicity after ionizing radiation suggests a relatively high radio-resistance [14]. A study by Oliver et al [15] found that in comparison with primary osteoblasts MSCs have a higher DNA repair capacity. This suggests that the radio resistant clonogenicity of MSCs is due to efficient DNA repair mechanisms, rather than resulting from a tolerance of slowly cycling cells to unrepaired DNA breaks. In a previous study we investigated changes in DNA repair efficiency and genomic stability in murine MSCs during *in vitro* expansion [16]. There is a gradual loss of the ability to recognize both endogenous and radiation-induced DNA double-strand breaks. This impaired DNA damage response was associated with reduced ATM dependency of foci formation, slower DNA repair kinetics, and an increased number of residual DNA repair foci. To gain a more detailed insight into these potentially deleterious age-related changes we have

conducted a whole-transcriptome comparison between *in vitro* aged and young human BM- MSCs. The observed dysregulation of key players in DNA double-strand break repair by homologous recombination was confirmed using gene expression studies as well as cell-based DNA repair assays after X-irradiation.

Methods

Transcriptomic analysis of in vitro aging hMSCs

BAM files of GSE59966 were downloaded from the GEO database [17]. Details of cell origin, *in vitro* aging, RNA extraction and RNA_Seq can be found in the original paper [17]. SAMTOOLS was applied to obtain FASTQ files [18]. FASTQC was applied to estimate the read quality of the FASTQ file [19]. R software (version: 3.5.3) was used for all the analyses in this study. ‘GenomicAlignments’ package was used to align short reads to a reference genome (human genome hg19). summarizeOverlaps function was applied to obtain the counting matrix. Since the library was prepared by a paired end technology, the parameter for alignment was chosen as “paired-end”. Counting model “Union” was chosen as the parameter in the function to indicate those reads which overlap any portion of exactly one feature are counted. ‘DEseq2’ package was applied to perform the differently expressed gene (DEG) analysis [20]. The Gene ontology (GO) analysis and KEGG pathway analysis was performed by clusterProfiler package [21]. The gene set enrichment analysis (GSEA) was done by GSEA software from Broad institute. IPA (Qiagen, Hilden, Germany) was applied to analyze the canonical pathways.

Cell isolation and culture

Bone marrow derived human MSCs were isolated from femoral heads of healthy donors recruited at the Clinic for General, Trauma and Reconstructive Surgery of the Ludwig-Maximilian University. The study was approved by the LMU ethical commission (project number 238/15) and performed according to the Declaration of Helsinki. All donors signed a written informed consent, declaring that any surplus tissue can be used for medical studies at the university hospital. Cells were isolated by washing the bone graft material with phosphate

buffered saline (PBS, pH 7.4). Furthermore, the bone material was incubated with 250 U/ml collagenase II (Worthington) in DMEM (Life Technologies) three times for 10 min at 37°C. To remove bone fragments, both suspensions were filtered with a 100 µm cell strainer. After centrifugation at 500×g for 5 min, the cell pellet was resuspended in culture media of αMEM (Thermo Fisher Scientific) supplemented with 10% fetal bovine serum (FBS, Life Technology) and 40 IU/ml penicillin/streptomycin (Life Technology). Cells were kept growing at 37°C in a humidified incubator at 5% CO₂ and ambient oxygen. After three days in culture, non-adherent cells were removed by washing with PBS for three times. For *in vitro* expansion and aging of the hBM-MSCs, cells were passaged every 7 days over a period of 10 weeks in antibiotic-free growth medium (see above). From week 2 till week 6, cells were split in a 1:3 ratio, and from week 7 till week 10 in a 1:2 ratio. The entire aging protocol therefore covered 8 passages, and from the splitting ratios can be estimated to be equivalent to approximately 10.3 cell divisions. Cells of passage 3 are used as “young MSCs” and cells of passage 11 as “*in vitro* ageing MSCs”, both for mRNA quantification by qRT-PCR and for immunofluorescence staining. Due to the requirement for a larger cell number, cell cycle analysis and measurement of BrdU incorporation was done on cells after one or two additional passages. Therefore, “young MSCs” refers to passage 3 to 4 and “ageing MSCs” refers to cells at passage 12 to 13 for these two assays.

RNA extraction and reverse transcription

Three days after the last passage, the cultured MSCs were washed twice with cold PBS. MSCs were collected using a cell scraper and centrifuged to obtain cell pellets. MAXWELL miRNA kit (Promega, Madison, WI) were used to extract total RNA on a Maxwell 16 AS2000 instrument (Promega, Madison, WI) . For reverse transcription, 100ng of RNA was processed with the SuperScript® III kit (Thermo Fisher, Waltham, MA) according to the manufacturers protocol with random hexamer and oligo-dT primers.

qRT-PCR

qRT-PCR reaction mix containing the 2µl cDNA template, 1µl (5pmol/µl) primers (table S1), 10µl PowerUp SybrGreen master mix (Thermo Fisher, Waltham, MA) and 7µl millipore water

was pipetted in three technical replicates and run in 96 well plates on a StepOnePlus instrument (Applied Biosystems, Foster City CA). The real-time cycling conditions were adjusted according to the manufacturer's recommendation. Raw data were collected as .eds files and analyzed using StepOne software v2.3 with the $\Delta\Delta C_t$ method and GAPDH as housekeeping gene.

X-ray irradiation

X-ray irradiation was performed in a closed cabinet XStrahl RS225 device (XStrahl Ltd., Surrey UK) operating at 195 kVp, 1.14 Gy/min dose rate and 3 mm Al filter. Dose calibration was regularly done using LiF thermoluminescence. Cells were kept at ambient temperature during irradiation, and control cells were treated identically apart from not placing them inside the radiation source.

Immunofluorescence

The MSCs were plated on sterile glass slides (SuperFrost+, Carl Roth GmbH, Karlsruhe, Germany) two days before X-irradiation at 30% cell density. At the indicated time points after irradiation, medium was removed and the slides rinsed with cold PBS. After fixing the cells for 10 min at ambient temperature in Roti Histofix4.5 (Carl Roth GmbH, Karlsruhe, Germany), slides were incubated for 1 hour in PBS plus (BSA 1g, glycine 0.5g, PBS 100 mL) to block the unspecific binding of first antibody. Incubation with the first antibody (53BP1: Novus Biologicals, NB100-305, pBRCA1: Abcam ab90528, γ -H2AX: Millipore 05-636) diluted in PBS plus (Dilution ratio: 53BP1:1:200, pBRCA1: 1:200, and γ -H2AX: 1:400) was done in a humidified chamber overnight at 4 °C. The slides were then washed 3 × 15min in PBS, before incubating them with 150 μ L of secondary antibody solution. Secondary antibody solution was prepared by mixing Alexa fluor® 488 conjugated goat anti-rabbit IgG H&L or Cy3 conjugated goat anti-mouse IgG H&L antibody (both Jackson ImmunoResearch, West Grove, PA) in PBS plus in a 1:400 dilution. After 1 h incubation at room temperature in the dark the slides were washed again 3 × 15min in PBS. For counter-staining of nuclei the slides were covered with 150 μ L of a DAPI solution (0.3 μ M in PBS). After 10 min incubation at RT the DAPI solution was removed, slides rinsed 2x with PBS and

covered with Vectashield (Vectorlabs, Burlingame, CA) and glass coverslips. Fluorescence microscopy was done on a digital BZ-X microscope (Keyence, Itasca, IL). Foci were counted automatically using the Keyence BZ-II analyzer. For each experiment at least 50 cells were counted.

Analysis of cell cycle distribution and kinetics

For analysis of changes in the cell cycle distribution, MSCs at day 2 after plating were trypsinized, washed with 4ml ice-cold PBS, and spun down at 1,400 rpm for 5 minutes. Following removal of the supernatant, cells were resuspended in 4 mL of ice-cold 70% ethanol for 3 hours. The fixed cells were spun down at 1,400 rpm for 5 minutes and resuspended in 475 μ L PBS, plus 3.3 μ L RNaseA (30 mg/mL) and 25 μ L propidium iodide (1 mg/mL, both Sigma-Aldrich, Taufkirchen, Germany). Flow cytometry was done using a Beckton Dickinson LSRII, with 531nm green-yellow laser excitation and 610nm/20nm bandpass filter for the PI fluorescence emission. Signals from 5×10^5 cells were stored from the main forward and side scatter population, and cells of G1 and G2/M phase counted using Gaussian curve fitting for the 2n and 4n peak, whereas S-phase and apoptotic cells were quantified by subtracting G1 and G2/M from the original histogram.

For quantification of DNA synthesizing cells and S-phase kinetics, 10^4 MSCs were plated on sterile glass slides and incubated for 2 days in growth medium. BrdU (Sigma-Aldrich, Taufkirchen, Germany) was added to a final concentration 10 μ g/mL and cells allowed to incorporate the nucleotide analog for 0h, 24 h and 48 h under standard growth conditions. After the indicated incubation times, the slides were washed twice with PBS before staining for 15 min with Hoechst 33342 solution (20mM final concentration, Sigma-Aldrich, Taufkirchen, Germany). Using UV-fluorescence microscopy (see above), 200 cells from randomly selected areas of each slide were photographed and the number of bright versus dim stained nuclei counted.

Results

Bioinformatical analysis of young and aging human MSCs

RNA-seq was performed to filter out differentially expressed genes (DEGs). The quality of the sequencing was confirmed by FASTQC (data available on request). PCA plots of the dysregulated genes during *in vitro* aging of six hMSC samples showed that the individual samples clustered together before *in vitro* aging and formed a second cluster after aging (Fig. S1). A volcano plot of the mean values of the relative gene expression changes revealed that the aging process induced changes in the expression of 1308 genes (Fig. 1A) (Threshold set for an absolute Log₂ fold-change larger than 1 and a Q-value less than 0.05). The heat map of the age-related DEGs (Fig. 1B) displays the top 150 genes with the highest significance ranked according to their DEG values. Unsupervised hierarchical clustering of the DEGs derived from cells of different donors confirmed the homogeneity in young and aging hMSCs, respectively. KEGG pathway analysis of genes with expression changes above the threshold shows that cell cycle regulation, cell senescence and DNA repair-related pathways are the most important dysregulated pathways during aging (Fig. 1C and Supplementary file 1: gene list). GO analysis of biological process, molecular function and cellular process of 1308 significantly dysregulated genes returned enriched sets of molecular functions to cellular processes of organelle fission, chromosome segregation, nuclear division and other chromosome related processes during *in vitro* aging (Fig. 2A-2C). Taken together the GO and KEGG analysis suggests that apart from already known pathways involved in stem cell aging, changes in DNA repair and chromosome construction pathways are also affected by the *in vitro* aging process of hMSCs.

Gene set enrichment analysis (GSEA) identified DNA repair, G2M checkpoints, E2F target, c-MYC targets, and oxidative phosphorylation as being influenced by *in vitro* aging (Fig. 3A). A heat map of the relative changes in DNA repair-related gene expression (Fig. 3B) revealing that most genes involved in DNA repair processes were down regulated.

Downregulation of genes involved in homologous recombination repair

In GSEA we found DNA repair to be dysregulated during aging (Fig 3A) and KEGG analysis suggested an effect on homologous recombination (Fig. 1C). The components involved in

homologous recombination repair were examined and several key players (*RAD51*, *RAD54B*, *RAD54L* and *BRCA1*) were found to be strongly downregulated (Fig. 3C-E). qRT-PCR in hBM-MSCs confirmed a downregulation between 2.3 fold (*RAD54L*) and 4 fold (*RAD54B*) of these genes during their *in vitro* expansion between week 2 and week 10 (Fig. 3F). String network analysis placed *RAD51* and *BRCA1* as the central node of homologous recombination (Fig S2A). IPA canonical pathway analysis of the differentially expressed genes revealed that cellular processes of “cell cycle control of chromosomal replication” and “BRCA1-mediated DNA damage response” are the most significantly affected signaling pathways during *in vitro* aging of hMSCs (Fig. S2B).

Cell cycle distribution and kinetics of actively replicating cells

Flow cytometry analysis of cell cycle distribution in early versus late passage hMSCs indicates no systematic changes related to the duration of in-vitro aging (Fig. S3A). Of the three donors analyzed, the percentage of S+G2/M cells, which might influence the portion of cells using homologous recombination repair, was 23.92%, 28.84%, and 22.18% in the early passages, and 27.57%, 24.80% and 23.34% in the late passage, respectively (Fig. S3B). Analysis of active DNA synthesis in S-phase using BrdU incorporation and Hoechst33342 quenching shows that, within 24 hours, (20.8 +/- 2.1)% of early passage MSCs and (17.8 +/- 1.5)% of late passage MSCs complete S-phase. During 48 h, the percentage of DNA synthesizing cells increased to (37.1 +/- 2.2)% or (35.6 +/-4.8)% in the early and late passages, respectively (difference not significant) (Fig. S4A-4B). Although there appears to be a fraction of > 50% slowly or not cycling cells, the comparison shows that this is unrelated to the passage number *in-vitro*.

Impaired DNA damage response during hMSC aging in vitro

To test whether the observed reduction in the expression of genes involved in homologous recombination has a functional consequence for DNA repair in *ex vitro* expanded MSCs we stained hBM-MSCs X-irradiated from different passage numbers for γ -H2AX/53BP1 double-

strand break repair foci (Fig. 4A). The mean number of γ -H2AX/53BP1 foci 2h after 3 Gy irradiation was 16.5 (CI 15.8 – 17.2) in young and 12.3 (CI 11.4 – 13.2) in aged cells ($p < 0.01$). Sham-irradiated cells of the same passage did not exhibit a significant difference in the background level of γ -H2AX/53BP1 foci (Fig. 4B). A higher proportion of unrepaired foci were seen to be retained in *in vitro* aged hBM-MSCs (46.1%) compared to young cells (28.2%) 24h after irradiation (Fig. 4C). These results confirmed the impairment of DNA damage sensing and repair during hMSC aging.

Changes in DNA repair foci involved in homologous recombination

Radiation-induced DNA double-strand breaks can be repaired by different pathways that are initiated by recognition of the damaged site and the rapid formation of γ -H2AX/53BP1 foci. As MSCs *in vitro* are proliferating they preferentially use homologous recombination to repair DNA DSBs. To measure DNA repair via homologous recombination the formation of pBRCA1 foci (alone or in co-localization with γ -H2AX) was compared in young and in *in vitro* aged hBM-MSCs (Fig. 5A). This confirmed that 2 hours after irradiation the older hBM-MSCs exhibited a lower number of pBRCA1+ γ -H2AX foci compared to younger hMSCs (Fig. 5B). A similar reduction with *in vitro* age was also seen for pBRCA1 and γ -H2AX foci counted separately (Fig. 5D-5G). The effective repair of DNA DSBs can be inferred by the subsequent disappearance of the DNA repair foci over a period of 24 hours. It was evident that a larger portion of DNA double-strand breaks remained unrepaired in *in vitro* aged versus the young hBM-MSCs (Fig. 5C, 5E, 5G). We also analyzed the distribution of the initial DNA repair foci in single cells. After 9 weeks in culture 16.5% of the MSCs belonged to a clearly separated subset of individual cells with reduced foci number (Fig. 5H-5I). These findings suggest that during ex-vivo expansion and aging of hBM-MSCs, a sub-population arises with a reduced DNA damage response.

Discussion

Cell-based therapies using mesenchymal stem cells require *in vitro* expansion prior to transplantation [22, 23]. The cellular aging that accompanies *in vitro* proliferation reduces both the capacity of the MSCs for colony formation and for lineage-specific differentiation [24]. However, there may also be a deleterious influence of *in vitro* aging on the capacity for genomic maintenance, essential for preventing an accumulation of cytogenetic damage. After successful transplantation the engrafted MSCs will be subject to genotoxic stress, e.g. from ionizing radiation in the form of natural low-dose background irradiation or from medical exposures. We have recently estimated that these exposure can accumulate to several hundreds of mGy over the life span of an adult stem cell [25]. A study by Ulyanenko et al provided evidence that gamma irradiation of hBM-MSCs using a low dose-rate exposure (0.1 mGy/min) was not sufficient to trigger a DNA damage response, whereas irradiation with the same total dose (300mGy) at an acute high dose-rate scheme (30mGy/min) strongly induced a cellular response [26].

In our previous study on DNA damage response in murine MSCs we found that the initial ATM-mediated recognition of DNA double-strand breaks formed after an exposure to ionizing irradiation was impaired after long-term ex-vivo cell expansion [16]. This impaired DNA damage response, indicated by a reduced number of initial γ -H2AX/53BP1 DSB repair foci, was associated with slower DNA repair kinetics and with an increase in the frequency of radiation-induced micro-nuclei. Consistent with the idea that impaired DNA repair increases the long-term risk for gene mutations leading to tumorigenesis [27] it has recently been found that cells derived from ex-vivo expanded rodent MSCs can undergo malignant transformation more frequently. MSCs of human origin reportedly are more resistant to transformation [28, 29]. It would therefore be interesting to determine if the resistance of human MSCs for *in vitro* transformation could be related to their DNA repair potential, and if so, how this is influenced by extended *in vitro* aging. Few studies have addressed DNA damage response (DDR) and DNA repair in human MSCs. Bigot et al found in their study that hypoxia (2% oxygen) during *in vitro* culture caused an

increased expression of proteins involved in HR repair (*BRCA1*, *RAD51* and *RBBP8*) and an upregulation of HR activity in hBM MSCs. Although hypoxia caused a reduced p53 activation at early passages in BM-MSCs following doxorubicin treatment, efficient recognition of DNA damage was observed. Doxorubicin is a DSB-inducing radiomimetic agent and is widely used as a cytotoxic drug in cancer treatment [11, 30], but its retention in cells is also influenced by the expression of membrane efflux pumps such as ABCG2. The high expression of ABCG2 in normal and malignant stem cells is an established and widely used marker leading to the excretion of DNA dyes (Hoechst 33342 side population) and export of cytotoxic molecules, thus reducing the intra-cellular concentration of such drugs [31-33]. Their experimental approach might therefore be confounded in part by changes in the stem-cell specific expression of detoxifying efflux pumps ABCG2, which is known to actively purge cells of doxorubicin. Ionizing radiation, in contrast is a more homogeneous inducer of DNA lesions, thus avoiding the bias of non-uniform drug concentrations in different cell types.

Therefore, we focused here on the dysregulation of DNA repair pathways in human MSCs after X-irradiation. Starting from a re-analysis of transcriptome changes during *in vitro* aging of hBM-MSCs using various bioinformatics tools we observed that gene networks involved in DNA repair by homologous recombination (HR) were impaired during the *in vitro* aging of human MSCs. Chromosome reconstruction and dysregulation of genes in DNA repair pathways were indeed associated with a reduction of DNA damage response in hMSCs. A lower number of γ -H2AX/53BP1 DSB repair foci may indicate a reduced initial DNA damage response in aged hBM-MSCs relative to young cells. We have discussed before that this is more likely an indicator of an impaired DDR rather than reflecting a lower number of breaks on the same DNA target level [16]. This was also in line with the observations that aged MSCs with lower number of initial γ -H2AX/53BP1 DSB repair foci developed more micro-nuclei after cell division.

Among several DNA repair pathways, HR involving BRCA1 has been identified here as the major process affected during *in vitro* aging of hBM-MSCs. This is also consistent with results from Ingenuity pathway analysis, which ranked “cell cycle control of chromosomal replication” and “BRCA1 mediated DNA damage control” as the 2 main processes affected. Since DNA repair by homologous recombination is specific for cells in the S- and G2 cell cycle phase, an influence of cell cycle control would be a natural consequence. We did not observe, however, significant

differences related to the passage number, neither in the cell cycle distribution of unirradiated hBM-MSCs nor in the percentage or kinetics of actively replicating cells. This might in part be the result of the short time between plating the cells and doing the various assays, thereby avoiding the accumulation of senescent cells. Another possible factor to be considered would be age-related differences in radiation-induced cell-cycle arrest. Our observation, however, that the difference between young and aged cells in the number of their radiation-induced 53BP1/ γ -H2AX and pBRCA1 foci was most pronounced at 2h after irradiation makes this idea unlikely.

Alterations in the way MSCs regulate the cell cycle most likely happen during the evolution of genetically unstable clones. Using a combination of clonal expansion of human MSCs with cytogenetic, CNV and transcriptome analysis, Wang et al found that a clone with aneuploidy and large number of CNVs displayed significant downregulation of cell cycle control, BRCA1-related DDR and ATM signaling, whereas in a clone without genetic alterations the same pathways were upregulated [29]. The clonal heterogeneity of age related dysregulation found in their study might underlie the formation of a subset of *in vitro* aged hBM-MSCs, which in the present report display a reduced DDR signal after X-irradiation.

DNA repair foci consisting of co-localized pBRCA1 and γ -H2AX protein foci specifically indicate sites of HR repair, and those foci appeared here with reduced frequency in X-irradiated aging hBM-MSCs as compared to irradiated young hBM-MSCs. It can be excluded that this is caused by a faster repair in aged cells, since they display a relatively higher fraction of unrepaired DNA double-strand breaks after 24 hours. In previous studies, homologous recombination has been linked to the radio-resistant phenotype of MSCs [12, 34]. Another study found that MSCs deficient in the Fanconi anemia protein FANCD2, which forms a complex during homologous recombination with BRCA1 and BRCA2, exhibited a higher level of DNA fragmentation between 1h and 24h after Cs137 gamma-irradiation, highlighting the importance of homology-directed double strand break repair specifically for those cells [35]. In our analysis, we observed that both homologous recombination and the Fanconi anemia pathway were affected during *in vitro* aging. The higher fraction of residual of pBRCA1+ γ -H2AX foci in *in vitro* expanded versus young hBM-MSCs suggests that *in vitro* aging had a detrimental impact not only on the recognition of DNA double-strand breaks, but also on the efficiency of their repair by homologous recombination. We also saw that in contrast to early passage hBM-MSCs, their aged

counterparts show a pronounced non-uniform pBRCA1+ γ -H2AX foci response after X-irradiation, with more than 50% of cells forming a distinct subset with less initial foci than expected from a random distribution. To find out if those with atypically low number of initial foci are related to cells showing less complete repair 24 hours later a time resolved study on individual cells would be required. But also without such a technically challenging method we can conclude that both the initial recognition of DNA breaks (via ATM signaling) and efficiency of HR are important for DNA repair in hBM-MSCs and that their *in vitro* aging can cause a reduction in both of them.

Conclusion

We confirmed that human MSCs from healthy donors also undergo a gradual reduction of DNA damage response during extended *in-vitro* growth. Of the several genes that were predicted by mRNA Seq and pathway analysis involved in DNA repair by homologous recombination, *BRCA1*, *Rad54* and *Rad51* were experimentally confirmed to show a significant downregulation. Analysis of pBRCA1+ γ H2AX foci after X-irradiation revealed that with increasing duration of *ex-vivo* growth, a subpopulation of cells develop that have a distinct lower capacity of damage recognition. It can therefore be concluded that human MSCs *in-vitro* show a similar age-related impairment of the DNA damage response as found previously in murine cells, and that the higher resistance hMSC against malignant transformation *in-vitro* must be due to other cellular processes.

Data accessibility: All primary data are available upon request. The result of the transcriptome analysis (List of genes with significant fold change) have been uploaded to the journal website (Supplementary_log2foldchange_1.csv)

Author Contributions: conceptualization, Michael J. Atkinson and Michael Rosemann; methodology, Michael Rosemann and Harry Scherthan; software, Xuanwen Bao; validation, Jing Wang; formal analysis, Xuanwen Bao; investigation, Michael Rosemann; resources, Attila Aszodi, and Veronika Schönitzer; data curation, Michael Rosemann and Xuanwen Bao; writing-original

draft preparation, Xuanwen Bao; writing-review and editing, Harry Scherthan, Attila Aszodi, Veronika Schönitzer and Michael Rosemann; visualization, Xuanwen Bao; supervision, Michael J. Atkinson and Michael Rosemann; project administration, Michael Rosemann; funding acquisition, Xuanwen Bao.

Acknowledgements: Parts of this study were financed by an EU FP7 grant for the collaborative project "RISK-IR" (EURATOM contract 323267). Xuanwen Bao was supported by a CSC scholarship (No. 201608210186). We are very grateful to the scientific impact from our former co-worker Dr. Jack Favor.

Conflicts of interests: The authors declare that they have no competing interests.

Reference

1. Aggarwal, S. & Pittenger, M. F. (2005) Human mesenchymal stem cells modulate allogeneic immune cell responses, *Blood*. **105**, 1815-1822.
2. Shigemoto-Kuroda, T., Oh, J. Y., Kim, D.-k., Jeong, H. J., Park, S. Y., Lee, H. J., Park, J. W., Kim, T. W., An, S. Y. & Prockop, D. J. (2017) MSC-derived extracellular vesicles attenuate immune responses in two autoimmune murine models: type 1 diabetes and uveoretinitis, *Stem cell reports*. **8**, 1214-1225.
3. Satija, N. K., Singh, V. K., Verma, Y. K., Gupta, P., Sharma, S., Afrin, F., Sharma, M., Sharma, P., Tripathi, R. & Gurudutta, G. (2009) Mesenchymal stem cell - based therapy: a new paradigm in regenerative medicine, *Journal of cellular and molecular medicine*. **13**, 4385-4402.
4. Maumus, M., Guérit, D., Toupet, K., Jorgensen, C. & Noël, D. (2011) Mesenchymal stem cell-based therapies in regenerative medicine: applications in rheumatology, *Stem cell research & therapy*. **2**, 14.
5. Alessio, N., Del Gaudio, S., Capasso, S., Di Bernardo, G., Cappabianca, S., Cipollaro, M., Peluso, G. & Galderisi, U. (2015) Low dose radiation induced senescence of human mesenchymal stromal cells and impaired the autophagy process, *Oncotarget*. **6**, 8155.
6. Höfig, I., Ingawale, Y., Atkinson, M. J., Hertlein, H., Nelson, P. J. & Rosemann, M. (2016) p53-dependent senescence in mesenchymal stem cells under chronic normoxia is potentiated by low-dose γ -irradiation, *Stem cells international*. **2016**.
7. Capasso, S., Alessio, N., Squillaro, T., Di Bernardo, G., Melone, M. A., Cipollaro, M., Peluso, G. & Galderisi, U. (2015) Changes in autophagy, proteasome activity and metabolism to determine a specific signature for acute and chronic senescent mesenchymal stromal cells, *Oncotarget*. **6**, 39457.

8. Choi, J.-S., Lee, B.-J., Park, H.-Y., Song, J.-S., Shin, S.-C., Lee, J.-C., Wang, S.-G. & Jung, J. S. (2015) Effects of donor age, long-term passage culture, and cryopreservation on tonsil-derived mesenchymal stem cells, *Cellular Physiology and Biochemistry*. **36**, 85-99.
9. Bork, S., Pfister, S., Witt, H., Horn, P., Korn, B., Ho, A. D. & Wagner, W. (2010) DNA methylation pattern changes upon long - term culture and aging of human mesenchymal stromal cells, *Aging cell*. **9**, 54-63.
10. Basciano, L., Nemos, C., Foliguet, B., de Isla, N., de Carvalho, M., Tran, N. & Dalloul, A. (2011) Long term culture of mesenchymal stem cells in hypoxia promotes a genetic program maintaining their undifferentiated and multipotent status, *BMC cell biology*. **12**, 12.
11. Bigot, N., Mouche, A., Preti, M., Loisel, S., Renoud, M. L., Le Guevel, R., Sensebe, L., Tarte, K. & Pedeux, R. (2015) Hypoxia Differentially Modulates the Genomic Stability of Clinical-Grade ADSCs and BM-MSCs in Long-Term Culture, *Stem cells (Dayton, Ohio)*. **33**, 3608-20.
12. Nicolay, N. H., Perez, R. L., Saffrich, R. & Huber, P. E. (2015) Radio-resistant mesenchymal stem cells: mechanisms of resistance and potential implications for the clinic, *Oncotarget*. **6**, 19366.
13. Sugrue, T., Lowndes, N. F. & Ceredig, R. (2013) Mesenchymal stromal cells: radio - resistant members of the bone marrow, *Immunology and cell biology*. **91**, 5-11.
14. Nicolay, N. H., Liang, Y., Perez, R. L., Bostel, T., Trinh, T., Sisombath, S., Weber, K.-J., Ho, A. D., Debus, J. & Saffrich, R. (2015) Mesenchymal stem cells are resistant to carbon ion radiotherapy, *Oncotarget*. **6**, 2076.
15. Oliver, L., Hue, E., Séry, Q., Lafargue, A., Pecqueur, C., Paris, F. & Vallette, F. M. (2013) Differentiation - related response to DNA breaks in human mesenchymal stem cells, *Stem cells (Dayton, Ohio)*. **31**, 800-807.
16. Hladik, D., Höfig, I., Oestreicher, U., Beckers, J., Matjanovski, M., Bao, X., Scherthan, H., Atkinson, M. J. & Rosemann, M. (2019) Long-term culture of mesenchymal stem cells impairs ATM-dependent recognition of DNA breaks and increases genetic instability, *Stem cell research & therapy*. **10**, 218.
17. Hänzelmann, S., Beier, F., Gusmao, E. G., Koch, C. M., Hummel, S., Charapitsa, I., Jousen, S., Benes, V., Brümendorf, T. H. & Reid, G. (2015) Replicative senescence is associated with nuclear reorganization and with DNA methylation at specific transcription factor binding sites, *Clinical epigenetics*. **7**, 19.
18. Li, H., Handsaker, B., Wysoker, A., Fennell, T., Ruan, J., Homer, N., Marth, G., Abecasis, G. & Durbin, R. (2009) The sequence alignment/map format and SAMtools, *Bioinformatics*. **25**, 2078-2079.
19. Andrews, S. (2010) FastQC: a quality control tool for high throughput sequence data in, Babraham Bioinformatics, Babraham Institute, Cambridge, United Kingdom,
20. Love, M. I., Huber, W. & Anders, S. (2014) Moderated estimation of fold change and dispersion for RNA-seq data with DESeq2, *Genome biology*. **15**, 550.
21. Yu, G., Wang, L.-G., Han, Y. & He, Q.-Y. (2012) clusterProfiler: an R package for comparing biological themes among gene clusters, *OmicS: a journal of integrative biology*. **16**, 284-287.
22. Golpanian, S., Wolf, A., Hatzistergos, K. E. & Hare, J. M. (2016) Rebuilding the damaged heart: mesenchymal stem cells, cell-based therapy, and engineered heart tissue, *Physiological reviews*. **96**, 1127-1168.
23. Pers, Y.-M., Rackwitz, L., Ferreira, R., Pullig, O., Delfour, C., Barry, F., Sensebe, L., Casteilla, L., Fleury, S. & Bourin,

- P. (2016) Adipose mesenchymal stromal cell - based therapy for severe osteoarthritis of the knee: A phase I dose - escalation trial, *Stem cells translational medicine*. **5**, 847-856.
24. Alt, E. U., Senst, C., Murthy, S. N., Slakey, D. P., Dupin, C. L., Chaffin, A. E., Kadowitz, P. J. & Izadpanah, R. (2012) Aging alters tissue resident mesenchymal stem cell properties, *Stem cell research*. **8**, 215-225.
25. Rosemann, M. (2016) Radiation-Induced Aging and Genetic Instability of Mesenchymal Stem Cells: An Issue for Late Health Effects? in *Genetics, Evolution and Radiation* pp. 385-396, Springer.
26. Ulyanenko, S., Pustovalova, M., Koryakin, S. & Beketov, E. (2019) Formation of gammaH2AX and pATM Foci in Human Mesenchymal Stem Cells Exposed to Low Dose-Rate Gamma-Radiation. **20**.
27. Kinzler, K. W. & Vogelstein, B. (1997) Cancer-susceptibility genes. Gatekeepers and caretakers, *Nature*. **386**, 761, 763.
28. Capelli, C., Pedrini, O., Cassina, G., Spinelli, O., Salmoiraghi, S., Golay, J., Rambaldi, A., Giussani, U. & Introna, M. (2014) Frequent occurrence of non-malignant genetic alterations in clinical grade mesenchymal stromal cells expanded for cell therapy protocols, *Haematologica*. **99**, e94.
29. Wang, Y., Zhang, Z., Chi, Y., Zhang, Q., Xu, F., Yang, Z., Meng, L., Yang, S., Yan, S. & Mao, A. (2013) Long-term cultured mesenchymal stem cells frequently develop genomic mutations but do not undergo malignant transformation, *Cell death & disease*. **4**, e950.
30. Bigot, N., Mouche, A., Preti, M., Loisel, S., Renoud, M. L., Le Guével, R., Sensebé, L., Tarte, K. & Pedeux, R. (2015) Hypoxia Differentially Modulates the Genomic Stability of Clinical - Grade ADSC s and BM - MSC s in Long - Term Culture, *Stem cells (Dayton, Ohio)*. **33**, 3608-3620.
31. Haslam, I. S., El-Chami, C., Faruqi, H., Shahmalak, A., O'Neill, C. A. & Paus, R. (2015) Differential expression and functionality of ATP-binding cassette transporters in the human hair follicle, *The British journal of dermatology*. **172**, 1562-1572.
32. Bunting, K. D. (2002) ABC transporters as phenotypic markers and functional regulators of stem cells, *Stem cells (Dayton, Ohio)*. **20**, 11-20.
33. Erdei, Z., Lorincz, R., Szebenyi, K., Pentek, A., Varga, N., Liko, I., Varady, G., Szakacs, G., Orban, T. I., Sarkadi, B. & Apati, A. (2014) Expression pattern of the human ABC transporters in pluripotent embryonic stem cells and in their derivatives, *Cytometry Part B, Clinical cytometry*. **86**, 299-310.
34. Cmielova, J., Havelek, R., Soukup, T., Jiroutová, A., Visek, B., Suchánek, J., Vavrova, J., Mokry, J., Muthna, D. & Bruckova, L. (2012) Gamma radiation induces senescence in human adult mesenchymal stem cells from bone marrow and periodontal ligaments, *International journal of radiation biology*. **88**, 393-404.
35. Berhane, H., Epperly, M. W., Goff, J., Kalash, R., Cao, S., Franicola, D., Zhang, X., Shields, D., Houghton, F. & Wang, H. (2014) Radiologic differences between bone marrow stromal and hematopoietic progenitor cell lines from Fanconi anemia (Fancd2^{-/-}) mice, *Radiation research*. **181**, 76-89.

Supporting Information

Fig. S1 PCA analysis showing the distribution of hMSC samples by their RNA transcriptom data.

Fig. S2 IPA analysis and gene network for the changed gene in *in vitro* aging process in hMSCs.

Fig. S3 Cell cycle analysis of P3/P4 and P12/P13 MSCs using propidium-iodide staining and flow cytometry.

Fig. S4 BrdU incorporation for 24h and 48h.

Supplementary file 1: List of the differentially expressed genes from dataset GSE59966 by their log₂-FC values.

Table S1: List and nucleotide sequence of primers used for qRT-PCR.

Figure legend

Fig. 1 DEG analysis for young and *in vitro* aging hMSCs. (A) Volcano plot showing DEGs between young hMSCs and *in vitro* aging hMSCs from GSE59966. (B) Heat map showing the most significant genes from GSE59966. (C) KEGG plot based on DEGs.

Fig 2. Gene ontology analysis for young and *in vitro* aging MSCs from GSE59966. (A) Gene ontology analysis for biological processes. (B) Gene ontology analysis for cellular components. (C) Gene ontology analysis for molecular functions.

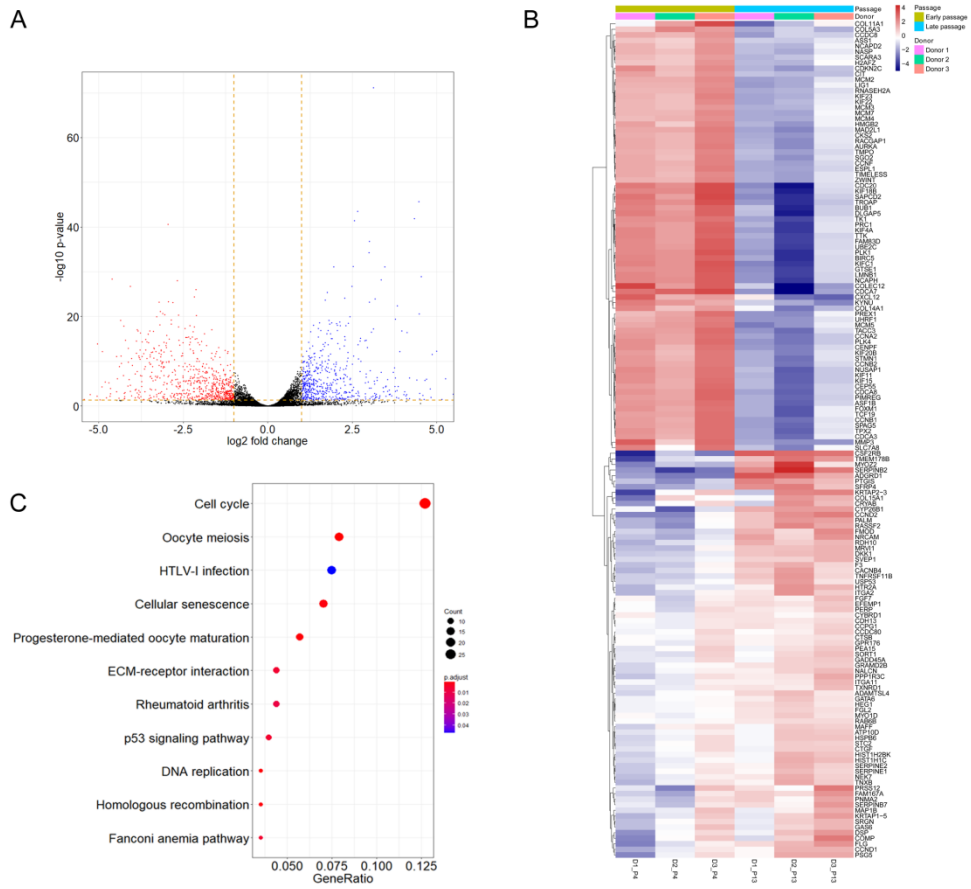
Fig. 3 Decreased expression of homologous recombination-related genes in *in vitro* aging hMSCs. (A) GSEA showing DNA repair and other enriched hallmarks between young and *in vitro* aging hMSCs from GSE59966. (B) The heat map for the significant DNA repair-related genes between young and *in vitro* aging hMSCs. (C) The decreased gene expression in *in vitro* aging hMSCs in RNA-seq showing by KEGG plot. (D) The most significantly changed homologous recombination-related genes between young and *in vitro* aging hMSCs by RNA-seq. The expression level change of BRCA1, RAD51, RAD54L, and RAD54B between young and *in vitro* aging hMSCs by RNA-seq (from GSE59966) (E) and RT-PCR (F). The expression of target genes in aging MSCs were set arbitrary to 1 (mean values \pm SEM, n = 3, *: p < 0.05, **: p < 0.01, significance by paired, one-sided T-test).

Fig. 4 Impaired DNA repair capacity in *in vitro* aging hMSCs. (A) DSB damage foci (γ H2AX, red; 53BP1, green) formation shown in young and *in vitro* aging MSCs in control, 2 hours and 24 hours after 3 Gy of γ -irradiation groups. Nuclear counterstaining by DAPI. Length of the scale bar: 1 μ m. (B) Quantification of γ H2AX+53BP1 DSB-foci in MSCs 2 hours and 24 hours after γ -irradiation. (C) The percentage of co-localized γ H2AX+53BP1 foci 24 hours post irradiation relative to the values at 2 hours post irradiation in young and *in vitro* aging MSCs (mean values \pm SEM, n = 3, *: p < 0.05, significance by paired, one-sided T-test).

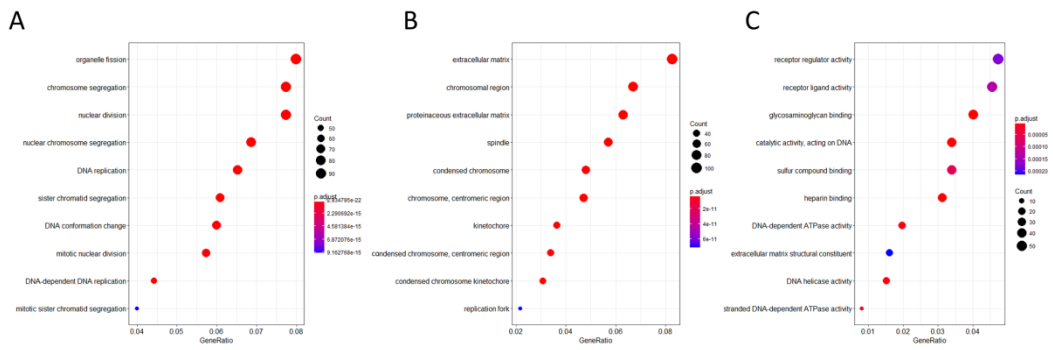
Fig. 5 Impaired homologous recombination repair capacity in *in vitro* aging hMSCs. (A) Repair foci formation is shown in young and *in vitro* aging hMSCs 2 hours and 24 hours after 3 Gy of γ -irradiation by immunofluorescence staining for pBRCA1 (red) and γ H2AX (green). Nuclear

Accepted Article

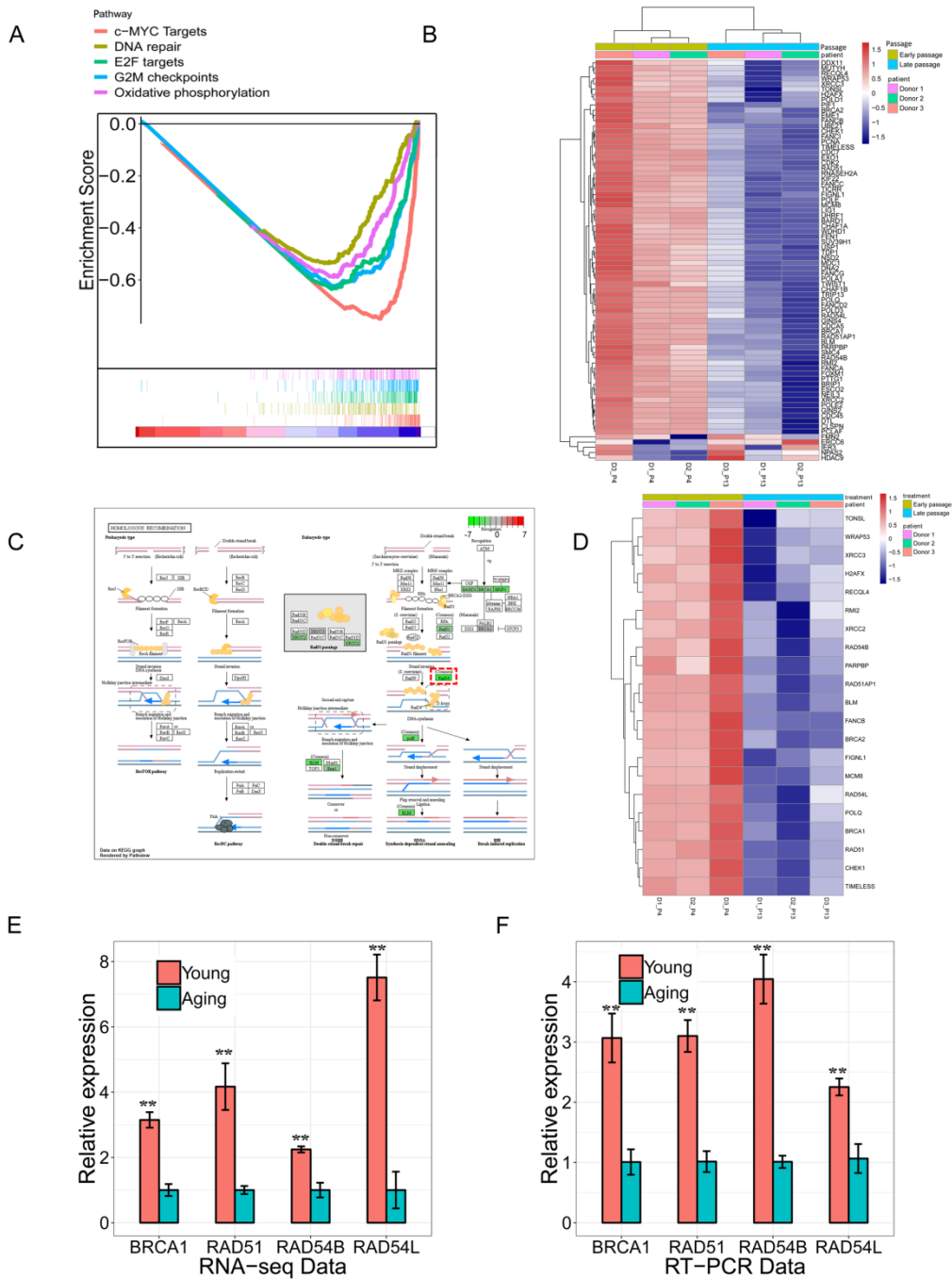
counterstaining by DAPI. Length of the scale bar: 1 μ m. (B) Quantification of pBRCA1+ γ H2AX - foci formation in hMSCs 2 hours and 24 hours after γ -irradiation. (C) The proportion of individual pBRCA1+ γ H2AX co-localizing foci in young and *in vitro* aging MSCs 24 hours after γ -irradiation. (D) Quantification of pBRCA1 foci formation in hMSCs 2 hours and 24 hours after γ -irradiation. (E) The proportion of pBRCA1 foci in young and *in vitro* aging MSCs 24 hours after γ -irradiation. (F) Quantification of γ H2AX foci in hMSCs 2 hours and 24 hours after γ -irradiation. (G) The proportion of individual γ H2AX foci in young and *in vitro* aging MSCs 24 hours after γ -irradiation. (H) Dispersion analysis of DNA repair foci in single cell from young hMSCs. (I) Dispersion analysis of DNA repair foci in single cells from *in vitro* aging hMSCs (mean values \pm SEM, n = 3, *: p < 0.05, significance by paired, one-sided T-test).



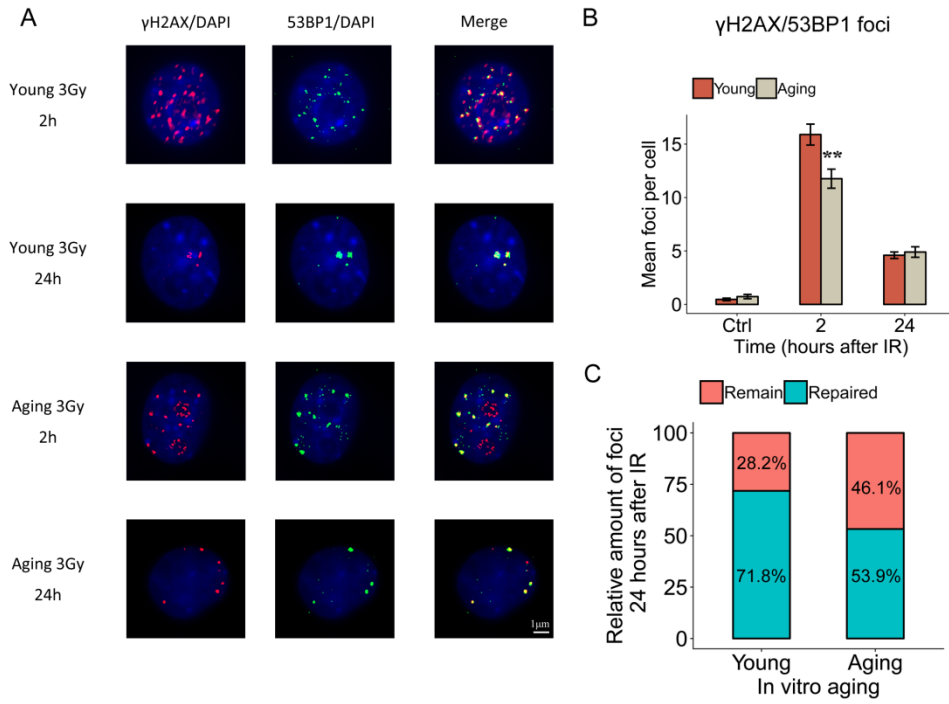
feb4_12867_f1.tif



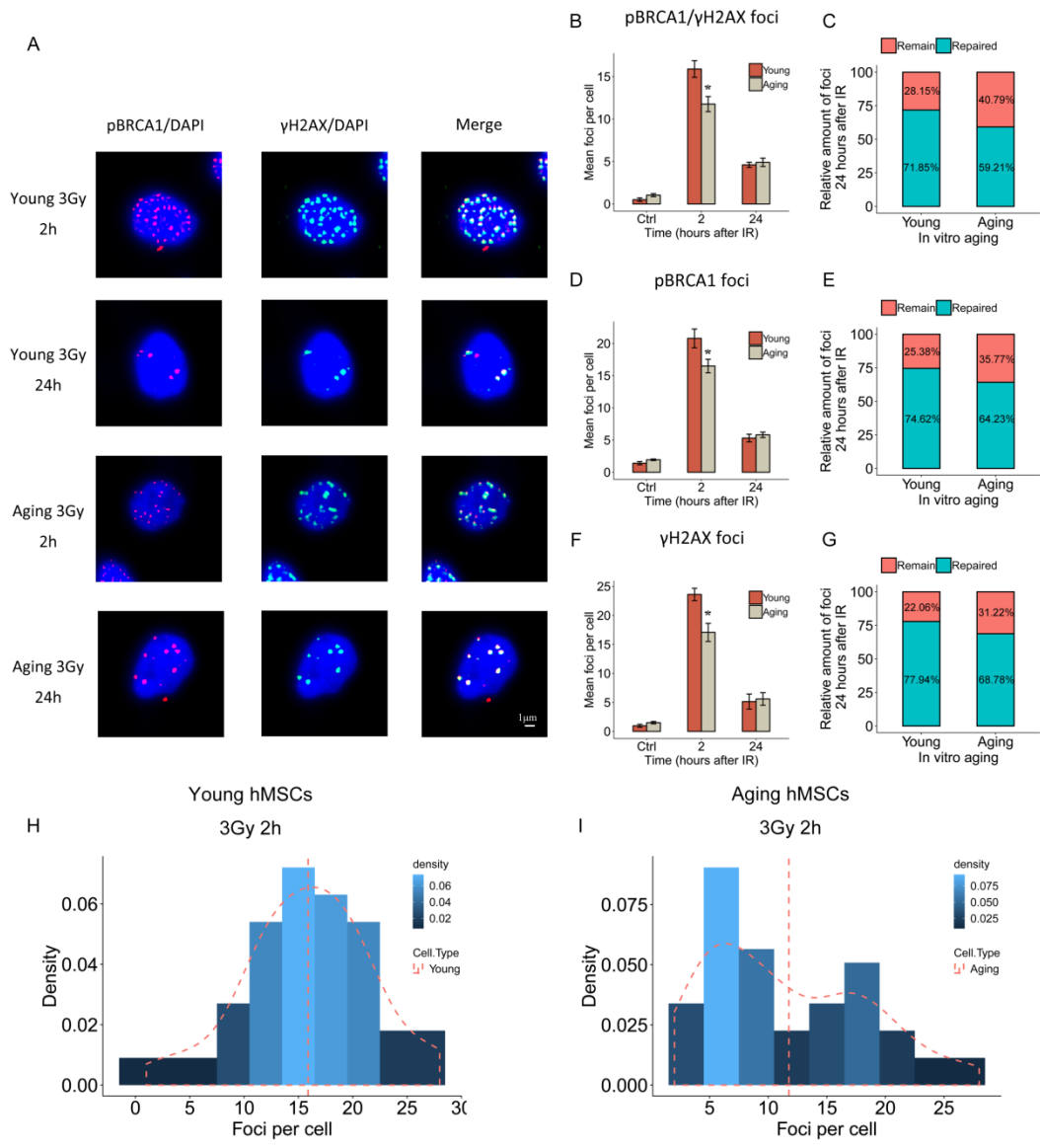
feb4_12867_f2.tiff



feb4_12867_f3.tif



feb4_12867_f4.tif



feb4_12867_f5.tif